HOKKAIDO UNIVERSITY

Title	Simulation of Peritectic Reaction during Cooling of Iron-Carbon Alloy
Author(s)	Matsuura, Kiyotaka; Kudoh, Masayuki; Ohmi, Tatsuya
Citation	ISIJ International, 35(6), 624-628 https://doi.org/10.2355/isijinternational.35.624
Issue Date	1995-06-15
Doc URL	https://hdl.handle.net/2115/75741
Rights	著作権は日本鉄鋼協会にある
Type	journal article
File Information	ISIJ Int. 35(6) 624.pdf

Hokkaido University Collection of Scholarly and Academic Papers : HUSCAP

ISIJ International, Vol. 35 (1995), No. 6, pp. 624–628

Simulation of Peritectic Reaction during Cooling of Iron–Carbon Alloy

Kiyotaka MATSUURA, Masayuki KUDOH and Tatsuya OHMI

Division of Materials Science and Engineering, Graduate School of Engineering, Hokkaido University, Kita-ku, Sapporo, Hokkaido, 060 Japan.

(Received on November 28, 1994; accepted in final form on January 27, 1995)

The effects of cooling rate on the growth behavior of austenite phase during cooling of an iron–carbon alloy are investigated by means of a numerical simulation. In the cooling process of this alloy, austenite phase nucleates at the interface between δ-ferrite and liquid phases at the peritectic temperature 1 768 K and then keeps growing during cooling. The growth mechanisms of austenite phase during cooling are: (1) carbon diffusion from liquid phase through austenite phase into δ-ferrite phase, (2) precipitaion from δ-ferrite phase, and (3) crystallization from liquid phase. All these mechanisms induce the growth of austenite phase with increasing cooling rate. The ratio of austenite phase which grows by precipitation and crystallization increases with increasing cooling rate, while that by carbon diffusion decreases. The decrease in the ratio of the diffusional growth is more remarkable for the migration of austenite/liquid interface than for that of δ-ferrite/austenite interface.

KEY WORDS: peritectic reaction; reaction rate; simulation; solidification; precipitation; transformation; diffusion; iron–carbon system.

1. Introduction

It is well known that peritectic reaction during solidification of carbon steel leads to generation of tensile stress on the surface of solidified steel shell,[1] segregation of alloying elements[2] and precipitation of inclusions such as manganese sulfide.[3] The tensile stress is a cause of cracking on the surface of continuously cast steel slabs, and the segregation and the precipitation affects the mechanical properties of steel products. An important guide for optimum control of these phenomena is considered to be the rate of peritectic reaction.

The present authors[4,5] have measured the rate of isothermal peritectic reaction in iron–carbon system by using a solid–liquid diffusion couple method, and have found that the peritectic reaction proceeds in accordance with the parabolic law and that the parabolic rate constant increases as temperature decreases. The former findings agrees with the diffusion-controlled theory,[6,7] while the latter is completely contrary to the general relationship between temperature and reaction rate. The rapid progress of peritectic reaction at lower temperatures, however, is understood to be caused by a larger extent of the carbon concentration range of austenite phase at lower temperatures, as seen in an iron–carbon binary equilibrium phase diagram[8]; the gradient of carbon concentration in austenite phase is steeper at lower temperatures, and this leads to a higher rate of carbon diffusion in austenite phase at lower temperatures.

In the present study, the process of peritectic reaction during cooling is simulated by using the relationship between temperature and isothermal peritectic reaction rate, and the effects of cooling rate on the growth behavior of austenite phase is investigated.

2. Procedure

2.1. Modelling of γ-Phase Growth

In the isothermal peritectic reaction of an iron–carbon alloy, austenite phase (γ) grows into both δ-ferrite phase (δ) and liquid phase by carbon diffusion from liquid phase through γ-phase into δ-phase, according to the diffusion-controlled theory.[6,7] On the other hand, in the cooling process of this alloy, the growth of γ-phase progresses with the precipitation from δ-phase and the crystallization from liquid phase as well as the diffusion of carbon. Therefore, in the present study, as shown in **Fig. 1**, continuous cooling process was simulated as repeating of the sequence of isothermal holding and quenching in a very small step both in time, Δt, and temperature, ΔT. The cooling rate, r, is expressed in Eq. (1).

$$r = \Delta T \Delta t^{-1} \quad \text{.....(1)}$$

The following assumptions are made for the present calculation.

(1) The growth of γ-phase occurs by carbon diffusion during isothermal holding for Δt and by precipitation and crystallization during quenching by ΔT.

(2) The parabolic rate constants obtained from the

© 1995 ISIJ

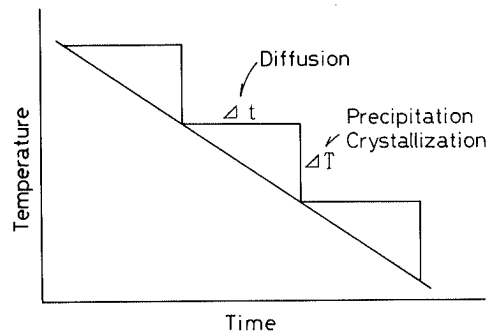

Fig. 1. Continuous cooling process simulated as a sequential combination of isothermal holding and quenching at very small steps in both time and temperature.

investigation of isothermal peritectic reaction are applicable to the diffusional growth during isothermal holding for Δt.

(3) No concentration gradients are present in δ-phase and liquid phase.

(4) The precipitation and crystallization of γ-phase occur without undercooling.

2.2. Growth of γ-Phase by Carbon Diffusion

The present authors[4,5] have investigated the growth behavior of γ-phase during isothermal peritectic reaction in iron–carbon system at various temperatures, and have obtained the relationship between temperature and parabolic rate constant, a. The parabolic rate constant is the coefficient in the parabolic law described in Eq. (2).

$$x = at^{1/2} \quad \text{.....(2)}$$

where x is the thickness of γ-phase (μm) and t is time (s). The value of the parabolic rate constant increases with decreasing temperature, as shown in **Fig. 2**, where both experimental and simulated results are included. The simulation was carried out by using the direct finite difference method[9,10] based on the diffusion-controlled theory.[6,7] As shown in Fig. 2, the parabolic rate constants for the migration of δ/γ interface and γ/liquid interface are well approximated by Eqs. (3) and (4), respectively

$$a_{\delta/\gamma} = 4.27(DC)^{1/2} \quad \text{.....(3)}$$

$$a_{\gamma/L} = 0.86(DC)^{1/2} \quad \text{.....(4)}$$

where D is the diffusion coefficient of carbon in γ-phase and C is the difference of carbon concentration in γ-phase at δ/γ interface from that at γ/liquid interface. They are expressed as functions of temperature in Eqs. (5)[10] and (6),[8] respectively.

$$D = 0.761 \times 10^8 \exp(-32\,160 R^{-1} T^{-1}) \quad (\mu m^2 s^{-1}) \quad \text{...(5)}$$

$$C = -7.545 \times 10^{-3} T + 13.34 \quad \text{(mass\%)} \quad \text{.....(6)}$$

where R is the gas constant (cal K^{-1} mol^{-1}) and T the absolute temperature (K).

The increment in thickness of γ-phase by the diffusional growth during isothermal holding for Δt is given in Eq. (7).

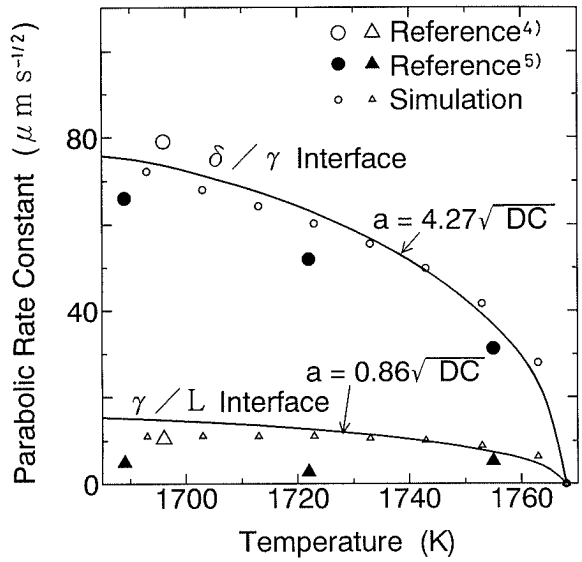

Fig. 2. Effect of temperature on the parabolic rate constant for the interface migration.
a: parabolic rate constant
D: diffusion coefficient of carbon in γ-phase
C: extent of carbon concentration range of γ-phase

$$\Delta x_{Dif} = (dx/dt)\Delta t \quad \text{.....(7)}$$

where dx/dt is the velocity of interface migration, obtained by differentiating Eq. (2).

$$dx/dt = a^2(2x)^{-1} \quad \text{.....(8)}$$

Then, one can obtain the increments in thickness of γ-phase by the migration of δ/γ interface and γ/liquid interface from Eqs. (9) and (10), respectively.

$$\Delta x_{Dif,\delta/\gamma} = a_{\delta/\gamma}{}^2(2x)^{-1}\Delta t \quad \text{.....(9)}$$

$$\Delta x_{Dif,\gamma/L} = a_{\gamma/L}{}^2(2x)^{-1}\Delta t \quad \text{.....(10)}$$

2.3. Growth of γ-Phase by Precipitation and Crystallization

Figure 3(a) shows a schematic profile of carbon concentration over δ, γ and liquid phases. Symbols C_1 through C_4 indicate the equilibrium carbon concentrations at the interfaces, which are shown in the schematic iron–carbon binary equilibrium phase diagram[8] of **Fig. 3(b)** and are given in Eqs. (11) through (14) as functions of temperature.

$$C_1 = 8.91 \times 10^{-4} T - 1.48 \quad \text{.....(11)}$$

$$C_2 = 1.68 \times 10^{-3} T - 2.81 \quad \text{.....(12)}$$

$$C_3 = -5.86 \times 10^{-3} T + 10.53 \quad \text{.....(13)}$$

$$C_4 = -1.83 \times 10^{-2} T + 32.89 \quad \text{.....(14)}$$

As a result of quenching from T to $(T-\Delta T)$, the carbon concentrations in δ-phase and γ-phase at δ/γ interface decrease from C_1 and C_2 to C'_1 and C'_2, respectively, as illustrated in Fig. 3(a). Simultaneously, the carbon concentrations in γ-phase and liquid phase at γ/liquid interface increase from C_3 and C_4 to C'_3 and C'_4, respectively.

The amount of carbon in δ-phase corresponding to the area symbolized as S_1 in Fig. 3(a) becomes excessive

© 1995 ISIJ

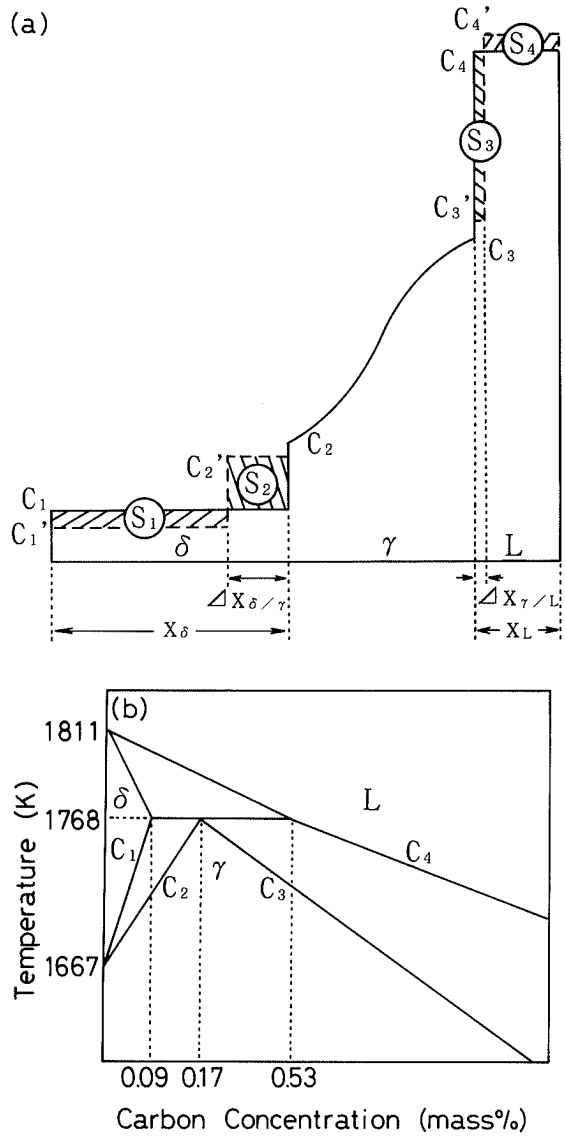

Fig. 3. (a) Profile of carbon concentration over δ, γ and liquid phases.
(b) Schematic iron–carbon binary phase diagram.[8]

owing to the decrease in the equilibrium carbon concentration of δ-phase from C_1 to C'_1. This amount of carbon is assumed to be consumed by the precipitation of γ-phase at δ/γ interface, which corresponds to the area symbolized as S_2 in Fig. 3(a). Therefore, from the condition that $S_1=S_2$, the thickness of γ-phase which precipitates on quenching by ΔT is expressed as Eq. (15).

$$\Delta x_{\delta/\gamma}=x_\delta(C_1-C'_1)/(C'_2-C'_1) \quad \text{.....(15)}$$

where x_δ is the thickness of δ-phase at temperature just before quenching by ΔT. Similarly, from the condition that $S_3=S_4$, the thickness of γ-phase which crystallizes at γ/liquid interface on quenching by ΔT is expressed as Eq. (16).

$$\Delta x_{\gamma/L}=x_L(C'_4-C_4)/(C'_4-C'_3) \quad \text{.....(16)}$$

where x_L is the thickness of liquid phase at a holding temperature just before quenching by T.

2.4. Conditions of Calculation

Calculation of the migration process of δ/γ and γ/liquid interfaces was carried out under the initial conditions given in Eq. (17).

$$\left.\begin{aligned} T&=1\,767\ \text{K}\\ x_\delta&=80\ \mu\text{m}\\ x_L&=20\ \mu\text{m}\end{aligned}\right\} \quad \text{.....(17)}$$

The ratio of the initial thickness of δ-phase to that of liquid phase given in Eq. (17) is nearly equivalent to the ratio of the initial volume fraction of δ-phase to that of liquid phase at the beginning of peritectic reaction during solidification of the iron–carbon alloy with a peritectic composition (0.17 mass% carbon).

The very short time for isothermal holding, Δt, was calculated by using Eq. (1) from the cooling rate, r, and the very small temperature difference for the quenching, ΔT. In the present calculation, $0<r\leqq 10$ (K s^{-1}) and $\Delta T=10^{-4}$ (s). The thickness of γ-phase at time, t, was calculate by using Eq. (18).

$$x|_{t=t}=x|_{t=t-\Delta t}+(\Delta x_{\text{Dif},\delta/\gamma}+\Delta x_{\text{Dif},\gamma/L})+(\Delta x_{\delta/\gamma}+\Delta x_{\gamma/L}) \quad \text{.....(18)}$$

The value of $x|_{t=t}$ is substituted into Eqs. (9) and (10) to calculate the increment in thickness by diffusional growth during the next time step, Δt. This calculation was continued until either x_δ or x_L decreases to zero.

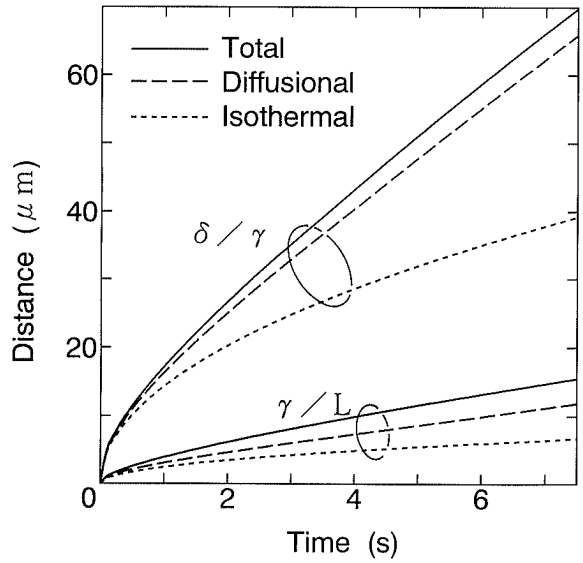

Fig. 4. Relationship between time and the migration distance of the interfaces.
Solid lines: cooled from 1 767 K at a rate of 1.0 K/s.
Broken lines: diffusional growth during cooling.
Dotted lines: isothermally hold at 1 767 K.

3. Results and Discussion

Figure 4 shows the relationship between time and the migration distance of the interfaces. The migration distance of both δ/γ and γ/liquid interfaces are longer in cooling from 1 767 K at a rate of 1.0 K/s (solid lines) than in isothermal holding at 1 767 K (dotted lines). The total migration distance during the continuous cooling (solid lines) is divided into the migration distance by the carbon diffusion (broken lines) and that by the precipitation and crystallization (distance between the solid and broken

© 1995 ISIJ

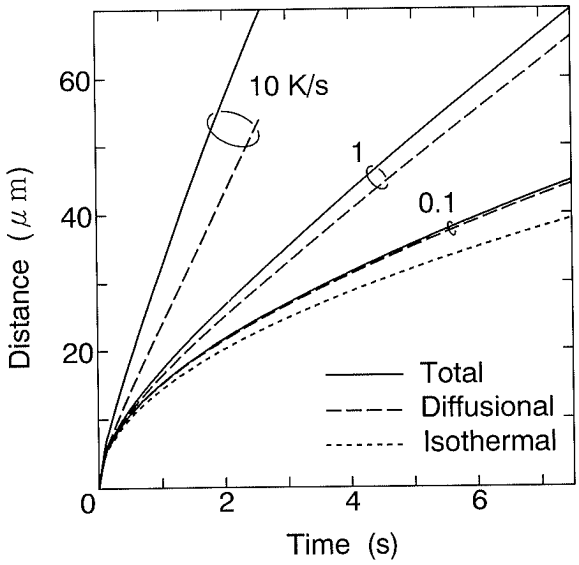

Fig. 5. Relationship between time and the migration distance of δ/γ interface at various cooling rates.

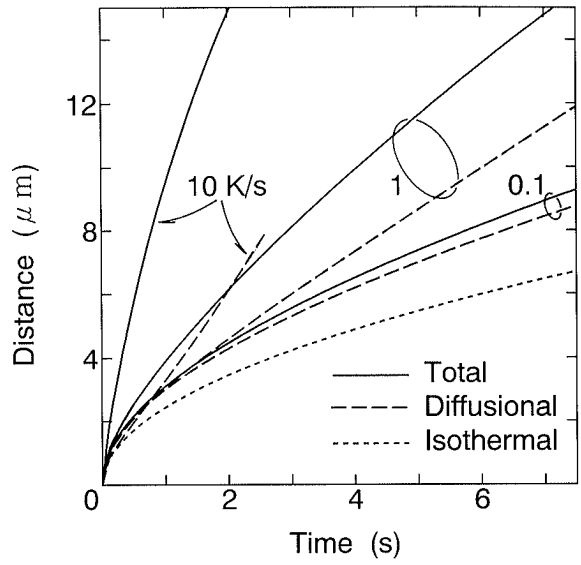

Fig. 6. Relationship between time and the migration distance of γ/liquid interface at various cooling rates.

lines), and the former is much longer than the latter.

As shown in Fig. 4, the migration of δ/γ interface is larger than that of γ/liquid interface, both during continuous cooling and isothermal holding. The similar results have been obtained from an experiment of isothermal peritectic reaction,[4,5] and the difference in migration distance between two types of interfaces has been explained from the difference between carbon concentrations at both interfaces[5]; the large difference in carbon concentration at γ/liquid interface induces a large amount of outward flow of carbon from liquid phase into δ-phase upon the slight migration of γ/liquid interface, while this amount of carbon flowing in is consumed in a large migration of δ/γ interface because of the small difference in carbon concentration at δ/γ interface.

Figure 5 shows the effect of cooling rate on the migration distance of δ/γ interface. Both the migration distance by carbon diffusion and that by precipitation increase with the cooling rate. Because the migration distance at various cooling rates are compared in reference to the same time axis in Fig. 5, the increase in cooling rate is equivalent to the decrease in temperature. Therefore, the increase in the migration distance by carbon diffusion with increasing cooling rate is explained by the fact that the gradient of carbon concentration in γ-phase is steeper at lower temperatures,[4,5] while the increase in the migration distance by precipitation with the cooling rate is explained by the decrease in the carbon solubility of δ-phase with decreasing temperature.

Figure 6 shows the effect of cooling rate on the migration distance of γ/liquid interface. The general tendency toward higher migration velocity at higher cooling rates is similar to the results shown in Fig. 5. The absolute values, however, are smaller in Fig. 6, and the increase in the migration distance by crystallization (distance between the solid and broken lines) shown in Fig. 6 is larger than that by precipitation shown in Fig. 5.

Figure 7 shows the effect of cooling rate on the ratio of the diffusional growth of γ-phase to the total growth

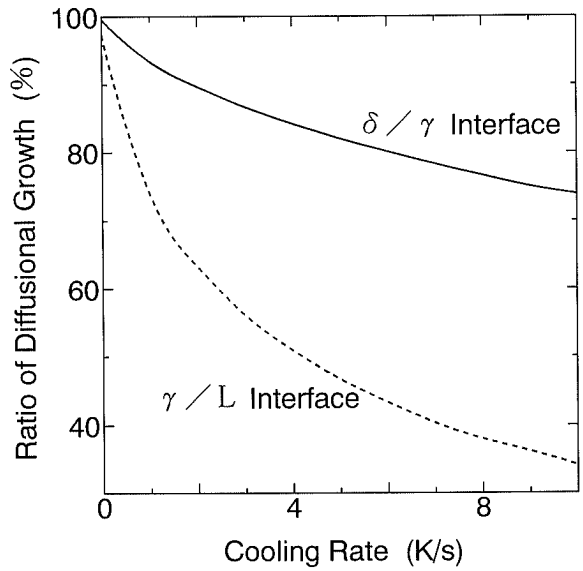

Fig. 7. Effect of cooling rate on the ratio of diffusional growth to the total growth of γ-phase.

shown by solid lines in Figs. 5 and 6. The ratio decreases with increasing cooling rate for both interfaces. However, the value of the ratio for γ/liquid interface is smaller. This may be explained as follows.

The fraction of γ-phase precipitating from δ-phase and that crystallizing from liquid phase are given in Eqs. (19) and (20), respectively, according to the lever rule based on an iron–carbon binary equilibrium phase diagram[8] (Fig. 3-(b)).

$$p_P=(C_{0\delta}-C_1)/(C_2-C_1) \quad \text{.....(19)}$$

$$p_C=(C_4-C_{0L})/(C_4-C_3) \quad \text{.....(20)}$$

where $C_{0\delta}$ is the initial carbon concentration of δ-phase and C_{0L} is that of liquid phase, and the values of them are 0.09 and 0.53 mass%, respectively. One can calculate the relationships between these fractions and temperature from Eqs. (19) and (20) and Eqs. (11) through (14). In the results shown in **Fig. 8**, p_C is larger than p_P in the

© 1995 ISIJ

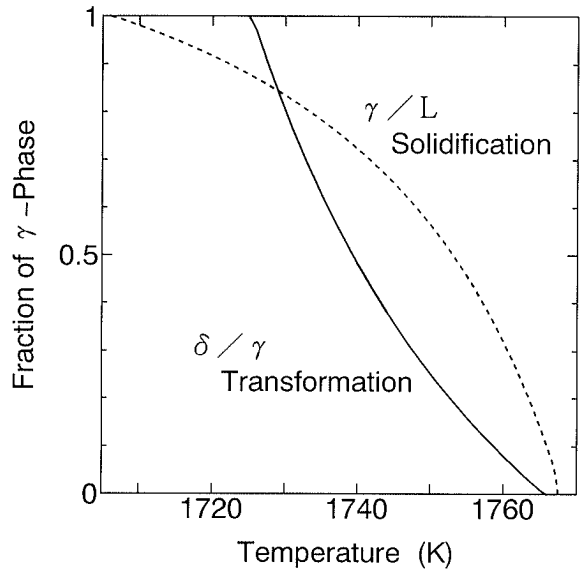

Fig. 8. Fraction of γ-phase precipitating from the δ-phase, p_P, and that crystallizing from the liquid phase, p_C, at various temperatures.

temperature range of about 40 K from the onset of peritectic reaction. Because, in the present simulation, the widest temperature range where peritectic reaction progressed is approximately 20 K, p_C is always larger than p_P. This may be one of the principal cause for the results shown in Fig. 7.

It is shown in Figs. 4 through 7 that a small quantity of γ-phase precipitates from δ-phase or crystallizes from liquid phase. In the present simulation, all the amount of this type of γ-phase is considered to precipitate at δ/γ interface or crystallize at γ/liquid interface and to contribute to the growth of γ-phase which is formed between δ and liquid phases and is growing by carbon diffusion. However, some quantity of this type of γ-phase may precipitate or crystallize away from the interfaces, when the cooling rate is very high, or when the size of δ-phase or liquid phase is very large. The mechanism and kinetics of the growth of this type of γ-phase is important as well as the diffusion-controlled mechanism[6,7] for the consideration of peritectic reaction during cooling. Calculation of peritectic reaction by taking account of this phenomena is considered to be significantly important in the future.

4. Conclusions

The process of peritectic reaction during cooling of an iron–carbon alloy has been simulated, and the effect of cooling rate on the growth behavior of γ-phase has been investigated. The results are summarized as follows.

The growth of γ-phase progresses with the precipitaion from δ-phase and the crystallization from liquid phase as well as the diffusion of carbon. All these mechanisms induce the growth of γ-phase with increasing cooling rate. The ratio of γ-phase which grows by precipitation and crystallization increases with increasing cooling rate, while that by carbon diffusion decreases. The decrease in the ratio of the diffusional growth is more remarkable for the migration of γ/liquid interface than for δ/γ interface.

Acknowledgements

The authors gratefully acknowledge the financial support of the Iron-and-Steel Research Promotion Fund for 1994 fiscal year from The Iron and Steel Institute of Japan in performing this study, and they are very grateful to Professor Kuniyoshi Ishii and Assistant Professor Youichi Itoh of Hokkaido University for their valuable discussion.

REFERENCES

1) T. Matsumiya, T. Saeki, J. Tanaka and T. Ariyoshi: *Tetsu-to-Hagané*, **68** (1982), 1782.
2) H. Fredriksson: *Scand. J. Metall.*, **5** (1976), 27.
3) Y. Itoh, N. Narita and K. Matsubara: *Tetsu-to-Hagané*, **67** (1981), 755.
4) K. Matsuura, Y. Itoh and T. Narita: *ISIJ Int.*, **33** (1993), 583.
5) K. Matsuura, H. Maruyama, Y. Itoh, M. Kudoh and K. Ishii: *ISIJ Int.*, **35** (1995), 183.
6) Y. Chuang, D. Reinisch and K. Schwerdtfeger: *Metall. Trans. A*, **6A** (1975), 235.
7) H. Fredriksson and S. Stjerndahl: *Met. Sci.*, **16** (1982), 575.
8) T. B. Massalski: Binary Alloy Phase Diagrams, Vol. 1, ASM, Materials Park, (1990), 842.
9) I. Ohnaka: *Tetsu-to-Hagané*, **65** (1979), 1737.
10) Y. Ueshima, S. Mizoguchi, T. Matsumiya and H. Kajioka: *Metall. Trans. B*, **17B** (1986), 845.

© 1995 ISIJ